

Fabrication of Hierarchical Hybrid Structures Using Bio-Enabled Layer-by-Layer Self-Assembly

Marketa Hnilova,¹ Banu Taktak Karaca,^{1,2} James Park,¹ Carol Jia,¹ Brandon R. Wilson,¹ Mehmet Sarikaya,¹ Candan Tamerler¹

¹Department of Material Science and Engineering, Genetically Engineered Materials Science and Engineering Center (GEMSEC), University of Washington, Seattle, Washington 98195; telephone: 206-616-6980; fax: 206-543-3100; e-mail: candan@u.washington.edu

²Department of Molecular Biology and Genetics, Istanbul Technical University, Istanbul, Turkey

Received 11 July 2011; revision received 15 November 2011; accepted 28 November 2011

Published online 14 December 2011 in Wiley Online Library (wileyonlinelibrary.com). DOI 10.1002/bit.24405

ABSTRACT: Development of versatile and flexible assembly systems for fabrication of functional hybrid nanomaterials with well-defined hierarchical and spatial organization is of a significant importance in practical nanobiotechnology applications. Here we demonstrate a bio-enabled self-assembly technique for fabrication of multi-layered protein and nanometallic assemblies utilizing a modular gold-binding (AuBP1) fusion tag. To accomplish the bottom-up assembly we first genetically fused the AuBP1 peptide sequence to the C-terminus of maltose-binding protein (MBP) using two different linkers to produce MBP-AuBP1 hetero-functional constructs. Using various spectroscopic techniques, surface plasmon resonance (SPR) and localized surface plasmon resonance (LSPR), we verified the exceptional binding and self-assembly characteristics of AuBP1 peptide. The AuBP1 peptide tag can direct the organization of recombinant MBP protein on various gold surfaces through an efficient control of the organic–inorganic interface at the molecular level. Furthermore using a combination of soft-lithography, self-assembly techniques and advanced AuBP1 peptide tag technology, we produced spatially and hierarchically controlled protein multi-layered assemblies on gold nanoparticle arrays with high molecular packing density and patterning efficiency in simple, reproducible steps. This model system offers layer-by-layer assembly capability based on specific AuBP1 peptide tag and constitutes novel biological routes for biofabrication of various protein arrays, plasmon-active nanometallic assemblies and devices with controlled organization, packing density and architecture.

Biotechnol. Bioeng. 2012;109: 1120–1130.

© 2011 Wiley Periodicals, Inc.

KEYWORDS: bio-enabled microarrays; gold nanoparticle; hetero-functional protein; layer-by-layer self-assembly; solid recognition

Introduction

Advanced nanostructured materials hierarchically assembled from functional inorganic and biological building blocks are of great interest to the broad scientific and engineering community due to the wide range of applications of these materials in the fabrication of devices, proteomics arrays and biosensors (Anker et al., 2008; Hammond, 2004; Qin et al., 2010; Seo et al., 2010; Tang et al., 2006). One of the main challenges to achieve desired organization is to control the biological–material interface in such a way that it will regulate the self-assembly process at the molecular level and, thus, will control the hierarchical formation of the 3D structural architecture and organization of functional inorganic and biological nanoscale assemblies. In the past few decades several deposition methods have been developed to fabricate multilayered molecular solid films, among these techniques are atomic layer deposition (Puurunen, 2005), Langmuir–Blodgett deposition (Schwartz et al., 1992); multilayer deposition based on use of various polymeric materials (Boudou et al., 2010) and self-assembled monolayers (SAMs) (Mrksich and Whitesides, 1996). Although these processes have been shown to be useful to fabricate various multilayered films and nanodevices, they still exhibit significant drawbacks, such as complexity of the process, long stacking time, low yield and stability, high cost, and limitations in material. Due to the requirement of harsh solvents and conditions the

Marketa Hnilova and Banu Taktak Karaca contributed equally to this work.

Correspondence to: C. Tamerler

Contract grant sponsor: NSF-MRSEC (GEMSEC) Program

Contract grant number: DMR#0520567

Contract grant sponsor: Turkish State Planning Organization

Contract grant sponsor: NSF-BioMat Program

Contract grant number: DMR#0706655

Additional Supporting Information may be found in the online version of this article.

resulting fabricated nanosystems are often not compatible with biological molecules and hence have only partial practical applications in the biomedical field. Moreover, some of these drawbacks are also associated with non-efficient engineering or the need to link organic and inorganic interfaces (Rusmini et al., 2007; Tamerler et al., 2010).

Conventionally, biological macromolecules, for example, proteins, are covalently attached to the inorganic interface by either chemical cross-linking using SAMs or by direct chemi- or physi-sorption via non-specific electrostatic interactions with the solid surface. Both approaches, however, immobilize and display biological macromolecules in a random orientation due to limited control over the reactivity of the protein with the activated SAM or with the bare solid surface (Rusmini et al., 2007). Moreover, complex chemical surface modifications and/or cross-linking reactions frequently also alter the active structure of the biological molecules, resulting in a loss of functionality or altered stability (Brzoska et al., 1994; Zhen et al., 2006). It is evident, therefore, that efficient fabrication of advanced biomaterials and biomolecular arrays through layer-by-layer assemblies will require more robust coupling techniques and utilization of versatile biology-friendly linkers that are material-specific, modular and amenable to control over a prescribed structural architecture (Sarikaya et al., 2003; Tamerler et al., 2010).

In the last decade, an alternative immobilization and deposition technique has emerged using combinatorially selected peptides with high binding affinity to inorganic solid surfaces that overcome many of the limitations of conventional chemical methods described above (Krauland et al., 2007; Sarikaya et al., 2003; Whaley et al., 2000). Inorganic-binding peptides selected from phage (Smith, 1985) or cell surface display (Boder and Wittrup, 1997) libraries have been developed and these peptides have the capability of controlling the assembly of nanostructures and biomolecules in various practical applications in nanoscience and technology (Brown et al., 2000; Dai et al., 2005; Lee et al., 2002b; Naik et al., 2002; Oren et al., 2007; Pacardo et al., 2009; Sano and Shiba, 2003; Whaley et al., 2000). Exceptional strong binding and self-assembly characteristics of inorganic-binding peptides onto solid surface interfaces offer versatile molecular linker alternatives enabling controlled layer-by-layer immobilization of biomolecules and nanostructures onto a wide range of solid supports useful to materials and biomedical applications. Most recently our and other groups have pioneered the utility of these inorganic-binding peptides in association with fusion partners, such as proteins or peptides, to build a hetero-functional units as molecular building blocks for a variety of directed self-assembly applications (Dai et al., 2005; Kacar et al., 2009; Khatayevich et al., 2010; Krauland et al., 2007; Sengupta et al., 2008). In previous reports, we showed that these specific inorganic-binding peptide tags are effective for site-directed protein immobilization on solid surfaces (Kacar et al., 2009; Sedlak et al., 2010;

Tamerler et al., 2010; Yuca et al., 2011). The peptide-tag approach offers significant advantages compared to immobilization techniques utilizing non-specific interactions of side groups of histidine and cysteine-tagged amino acids with metallic surfaces, for example, gold, silver and nickel (Kumara et al., 2007; Park et al., 2009; Slocik et al., 2005; Zheng et al., 2010).

Here we demonstrate bio-enabled self-assembly technique for fabrication of hybrid metallic nanostructures and protein arrays with multilayer hierarchical architecture. Specifically we show the utility of combinatorially selected gold-binding peptide (AuBP1) (Hnilova et al., 2008) as a modular tag which is fused either to a model protein or peptide molecules. A high-affinity AuBP1 peptide tag sequence used in this study was generated from a diverse peptide library using optimized combinatorial approaches adapted by our group (Hnilova et al., 2008). In the present work modular AuBP1 peptide tag enables the immobilization of multiple layers of nanostructures and fusion proteins onto gold surface using a combination of soft-lithography and self-assembly techniques. Using this experimental strategy, we first produced a bi-functional molecule by genetic fusion of AuBP1 peptide tag to the C'-terminus of maltose-binding protein (MBP) using two structurally distinct spacers, that is, either rigid (PGPGPG) or flexible (SGGG) spacer. We then performed quantitative binding assays, using surface plasmon resonance (SPR) and localized surface plasmon resonance (LSPR). Spectroscopic evaluations confirmed similar levels gold-binding peptide functionality for both of the engineered MBP-AuBP1 derivatives. Moreover, these fusion proteins demonstrated considerable higher gold-binding affinities compared to wild type-MBP. Next, we tested the effectiveness of proposed bio-enabled layer-by-layer assembly process on a patterned glass surface. To accomplish assembly on a glass surface, we first conjugated AuBP1 to a glass binding peptide (QBP1), and patterned the surface with the resulting bi-functional peptide (AuBP1-QBP1). We then incubated the gold nanoparticles, which were assembled on the peptide patterns. A third layer of MBP-AuBP1 derivatives was immobilized selectively onto the gold nanoparticles decorating the glass surface. Finally, immobilized fusion protein localized on these assembled hybrid structures was detected with high precision by anti-MBP antibody labeled with a fluorophore.

The model fusion partners, QBP1 and MBP, were rationally selected to demonstrate the modular capacity of AuBP1 peptide tag technology as versatile and specific material linker. Both MBP and QBP1 fusion partner contain no cysteine minimizing the sulfide-induced non-specific peptide and protein interactions with metallic surfaces (Kumara et al., 2007; Park et al., 2009; Slocik et al., 2005; Zheng et al., 2010). This inherent biochemical characteristic enables the direct and quantitative study of the specific gold-binding capacity of model fusion constructs that can be directly attributed to AuBP1 fusion peptide tag. Our studies demonstrate that designed model multi-functional AuBP1-based derivatives have the capacity for controlling

and directing protein as well as nanostructure self-assembly on solid surfaces. Described AuBP1 peptide technology constitutes novel biological routes for biofabrication of various protein arrays, plasmon-active nanometallic assemblies, biosensing and nanophotonic devices with controlled organization and architecture.

Materials and Methods

Fusion Protein Construction and Expression

Synthetic oligonucleotides encoding to AuBP1, with either rigid PGPGPG or flexible SGGG spacers, were amplified using PCR and inserted into the *XmnI* and *PstI* sites of vector pMAL-c2x (New England Biolabs, Beverly, MA) to generate pMAL-PGPGPG-AuBP1 or pMAL-SGGG-AuBP1 plasmid constructs. Recombinant *E. coli* strain ER2507 harboring desired expression plasmid constructs were grown in LB medium. The expression of MBP-GFPuv-AgBP2C was induced by adding IPTG (isopropyl-beta-D-thiogalactopyranoside) at OD₆₀₀ of 0.5 to a final concentration of 0.3 mM. The expressed protein was purified on amylose resin (New England Biolabs, Beverly, MA) column following manufacturer's instruction. The protein samples were analyzed by 12% SDS-PAGE. The purity of eluted MBP protein fractions were further determined by SDS-PAGE electrophoresis and by mass spectrometry (MS). The sequences of the oligonucleotide primers, vectors, enzymes, strains, Maldi-TOF MS spectra and detailed description of cloning and expression procedures are given in Supporting Information.

Surface Plasmon Resonance (SPR) Binding Experiments

SPR measurements were conducted using a four-channel instrument (Radio Engineering Institute, Czech Republic). Solutions were degassed to avoid bubbles in the flow cell. First, PBS buffer solution was flowed over the surface until a stable baseline signal was established. Selected recombinant protein in PBS were used at concentrations between 0.025 and 0.2 μM, and allowed to flow over the gold surface while the adsorption was monitored. The temperature within the flow cell of the SPR was kept at constant 25°C. All solutions were introduced to the flow cell at a rate of 140 μL/s. The binding kinetics constants were analyzed by Student's *t*-test statistical analysis.

Production of Hybrid Gold Nanoparticles

Citrate-capped 15 nm gold nanoparticles (Au NP) (Ted Pella Inc., Redding, CA) were incubated with serial dilutions of MBP-AuBP1 fusion or wild type MBP (wt-MBP) proteins (1.0 to 0.001 μM) for 2 h at room temperature. The replacement of the citrate ions by protein molecules were monitored by measurement of LSPR band shift recorded using Saphire spectrophotometer (Tecan, San Jose, CA). To

remove the excess ligand, protein-functionalized Au NP were centrifuged at 13,000 rpm for 10 min and resuspended in DI water. The stability of the protein-functionalized Au NP was monitored in salt agglomeration assay by sequential addition of 5 M NaCl solution to the Au NP to a final concentration of 1 M. Au NP agglomeration was monitored by color change and by the shift of absorption bands recorded using Saphire spectrophotometer (Tecan). In agarose gel experiments, washed Au NP functionalized with serial protein concentrations, were loaded to a 0.5% (w/v) agarose gel. After 10 min migration in TAE buffer at 40 V the protein-stabilized nanoparticles were detected on the agarose gel as red bands and compared to non-functionalized particle samples. To further test the degree of protein modification, washed Au NP was functionalized with either 0.05 μM fusion MBP-AuBP1 or with wt-MBP proteins. The resulting mixtures were immobilized on a nitrocellulose membrane and the immobilized MBP protein was detected by a monoclonal anti-MBP-HRP conjugate (NEB) at 1:1,000 dilution and reacted with the TMS substrate (Pierce, Rockford, IL) to produce a colored product.

Fabrication of Protein Arrays

Gold film (25 nm thick) on silica wafer was evaporated onto pre-coated chromium layer (~3 nm thick) by electron beam evaporation. The gold surface (~1 cm × 1 cm) was subsequently cleaned by 5 min ultrasonication in methanol/acetone (1:1), isopropyl alcohol, and DI water followed by drying with nitrogen gas. Polydimethylsiloxane (PDMS) stamps were cleaned by 20 min ultrasonication in ethanol and DI water followed by nitrogen gas drying. MBP-AuBP1 constructs and wt-MBP (20 μM) were incubated on clean PDMS stamp for 10 min. Excess protein was removed and the stamp was gently dried with nitrogen gas. Gold surfaces were incubated with the protein-loaded stamps for 10 min followed by 1 min wash with DI water and nitrogen gas to dry the surface. The un-reacted gold surface was then blocked with 1% BSA PBS solution for 1 h followed by a 1 min wash and nitrogen gas drying. The immobilized MBP fusion proteins were visualized after 30 min incubation with anti-MBP (Zymed, San Francisco, CA) fluorescently pre-labeled using Zenon-Alexa-546 or Zenon-Alexa-488 labeling kit (Invitrogen, Carlsbad, CA) as follows: 2 μL of anti-MBP solution were mixed with 8 μL PBS and 5 μL of Zenon-Alexa IgG labeling dye and incubated for 30 min on ice followed by further dilution in 0.5 mL of PBS buffer. In final step substrate was gently washed for 1 min with DI water, dried, and imaged using a fluorescence microscope (Nikon, Yokohama, Japan) and Metamorph Software (Universal Imaging LLC, Burbank, CA).

Bio-Enabled Layer-by-Layer Fabrication of Arrayed Surfaces

To create the gold nanoparticle patterned surfaces, the GEPI bi-functional fusion peptide QBP1-AuBP1 (200 μg/ml) was

micro-contact printed on glass cover slide (Thermo Fisher Scientific, Waltham, MA) in the same manner as described above using 15 min incubation time. After the stamping and washing steps, the peptide-arrayed substrate was incubated with 15 nm Au NP for 30 min, washed for 1 min, and dried under nitrogen. MBP-AuBP1 or wt-MBP proteins were incubated on gold patterned surface for 1 h, followed by 1 min washing and nitrogen drying steps. The un-reacted surface was blocked with 1% (w/v) BSA in PBS and the immobilized proteins were immune-stained using the methods described above.

Result and Discussion

Design and Engineering of Hetero-Functional MBP-AuBP1 Fusion Protein Constructs

Based on our previous findings, we hypothesized that the specific peptide tag presented in the fusion protein constructs would increase the affinity, orientation and molecular organization for the self-assembled proteins on

the surfaces. To demonstrate the feasibility of our hypothesis, we engineered different fusion-protein derivatives of specific gold-binding peptide tag and maltose-binding protein (MBP) separated by two structurally different spacing motifs. It has been shown that the design of linkers separating two functional domains is crucially important for efficient production and fabrication of hetero-functional protein units (Fairman and Akerfeldt, 2005; George and Heringa, 2002; Tamerler et al., 2010; Wriggers et al., 2005). MBP fusion partner was rationally selected due to the lack of cysteine amino acids preventing the sulfide-induced non-specific protein interactions with gold surface. MBP protein is well studied and it is known to tolerate C-terminal genetic fusion as well as has high protein yield when expressed in bacterial cells. Specifically, we designed and successfully expressed the MBP-AuBP1 fusion construct containing either a rigid (PGPGPG)- or flexible (SGGG)-spacer separating the AuBP1 peptide tag from the MBP protein (Fig. 1a–c and Supporting Information). Either of the purified hetero-functional MBP-AuBP1 fusion proteins was then used to investigate the effect of the engineered AuBP1 peptide tag on protein adsorption

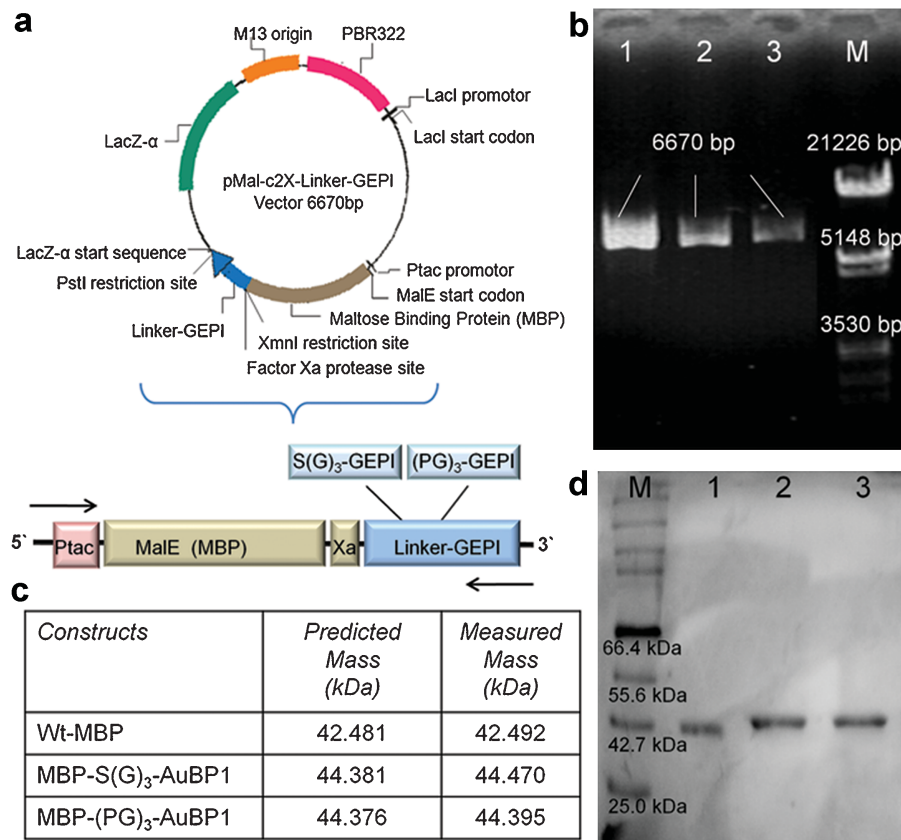


Figure 1. Vector construction and expression of fusion MBP-AuBP1 proteins. Schematic diagram of vector construct (**panel a**) and analysis on agarose gel (**panel b**), line (1), MBP-S(G)₃-AuBP1; line (2), MBP-(PG)₃-AuBP1 gene; line (3), control plasmid; line (M), lambda DNA markers of *Eco*RI + *Hind*III double digest. Mass spectroscopy (Maldi-TOF) analysis of expressed and purified fusion proteins with stiff or flexible linkers and wild type MBP (**panel c**) with respective SDS-PAGE (**panel d**); line (M), protein marker, line (1), wt-MBP; line (2), MBP-S(G)₃-AuBP1; line (3), MBP-(PG)₃-AuBP1. [Color figure can be seen in the online version of this article, available at <http://wileyonlinelibrary.com/bit>]

onto various forms of gold surfaces using biochemical, spectroscopic and molecular imaging techniques, as described in following sections.

Binding Affinity of Hetero-Functional MBP-AuBP1 on Flat Gold Surface

Here we used SPR spectroscopy to study the effect of engineered AuBP1 peptide tag present in hetero-functional MBP-AuBP1 fusions on protein–solid interactions and binding. Figure 2a shows an example of the experimental SPR sensograms recorded for MBP-(PG)₃-AuBP1 at various protein concentrations fitted with a Langmuir isotherm binding model. The apparent binding rates (k_{obs}) were derived from nonlinear curve fitting of the recorded SPR sensograms to the Langmuir binding isotherm as described earlier (Tamerler et al., 2006). The kinetic parameters of the adsorption and desorption process were further calculated from a linear regression: $k_{\text{obs}} = k_a C + k_d$, where

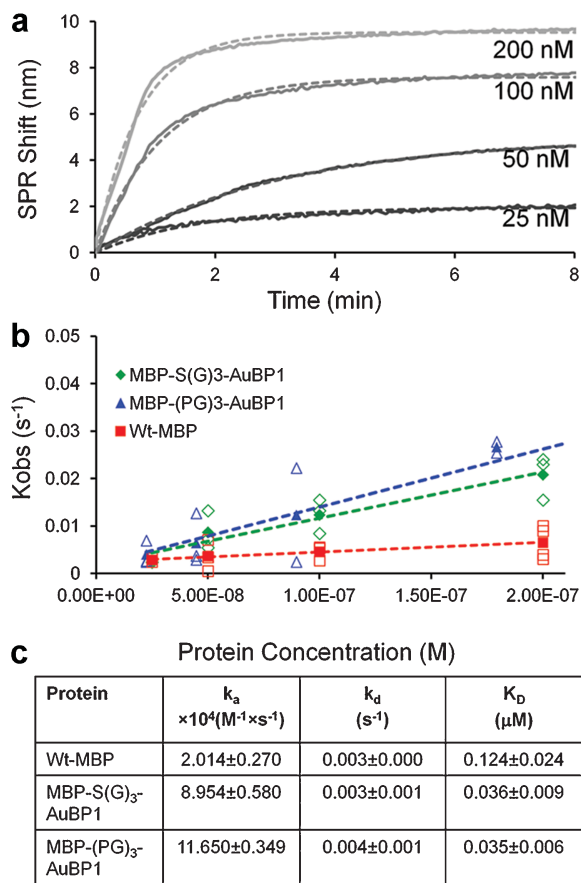


Figure 2. SPR binding analysis of expressed fusion proteins. Example of SPR sensograms recorded for MBP-(PG)₃-AuBP1 at various concentrations (panel a); k_{obs} plots for wild type MBP (red), MBP-S(G)₃-AuBP1 (green), MBP-(PG)₃-AuBP1 proteins (blue) (panel b); table of observed association (k_a) and dissociation (k_d) rate constants for fusion MBP proteins and respective calculated values of dissociation constants (K_D) (mean \pm SE) (panel c). [Color figure can be seen in the online version of this article, available at <http://wileyonlinelibrary.com/bit>]

C is the protein concentration, and k_a (slope) and k_d (intercept) are the association and dissociation rate constants, respectively (Fig. 2b). The dissociation constants (K_D) can be then calculated from $K_D = k_d/k_a$. The observed association rate constant k_a (mean \pm SE) values for fusion MBP-AuBP1 proteins $(8.95 \pm 0.58) \times 10^4 \text{ M}^{-1} \text{ s}^{-1}$ for MBP-S(G)₃-AuBP1 and $(11.65 \pm 0.35) \times 10^4 \text{ M}^{-1} \text{ s}^{-1}$ for MBP-(PG)₃-AuBP1 were considerably higher than the k_a obtained for the wt-MBP protein of $(2.01 \pm 0.27) \times 10^4 \text{ M}^{-1} \text{ s}^{-1}$ (Fig. 2c). The four- to sixfold enhancement in observed association rate constants for both hetero-functional fusion proteins compared to wt-MBP is statistically significant at $\alpha \leq 0.01$ in *t*-test and can be contributed to the enhanced binding affinity of the fusion protein to the gold surface through the incorporated AuBP1 peptide tag. On the other hand the AuBP1 tag did not affect the dissociation rate constants (k_d) tabulated in Figure 2c. Consequently, the corresponding calculated dissociation constant (K_D) values of both fusion MBP-AuBP1 proteins were significantly lower than the control wt-MBP (Fig. 2c). Overall, these observed differences in binding affinity constants indicate that both fusion MBP-AuBP1 derivatives have significantly higher binding affinity to gold compared to wt-MBP as well as suggest that AuBP1 peptide tag is similarly functional in both fusion proteins (Fig. 2c). Furthermore the observed nanomolar K_D values for these fusion proteins are comparable to our other fusion protein constructs and roughly correspond to adsorption parameters of alkanethiol molecules on gold surface used in conventional chemical approaches (Kacar et al., 2009).

Fabrication of Hybrid MBP-AuBP1 Gold Nanoparticles

Gold nanoparticles (Au NP) either immobilized on planar surfaces or dispersed in solution are of great interest in developing novel hybrid nanoscale diagnostics tools due to their strong LSPR properties (Iosin et al., 2009; Sedlak et al., 2010; Tullman et al., 2007). Stable and controlled modifications of Au NP surface with either functional proteins or recognition molecular probes are crucial prerequisite for their successful practical utility in *in vivo* and *in vitro* bioassays (Anker et al., 2008; Kacar et al., 2009; Levy et al., 2004; Nath and Chilkoti, 2004; Park et al., 2009). Here, the replacement of citrate ions by protein molecules on gold NP surface was tested by analyzing the LSPR spectrum shift upon exposure to our fusion proteins (0.001 to 2 μM). The pre-made 15 nm citrate-capped Au NPs (Ted Pella) exhibit a characteristic LSPR peak at $\sim 520 \text{ nm}$ wavelength which, upon protein–surface interaction and binding, demonstrate a red-shift. This shift is due to the local change of dielectric permittivity resulting from the formation of a protein layer on the surface of Au NP (Levy et al., 2004; Sedlak et al., 2010). Comparison of the observed LSPR shifts recorded at various protein concentrations (Fig. 3b–c) reveals that MBP-AuBP1 fusion proteins bind to Au NP with higher

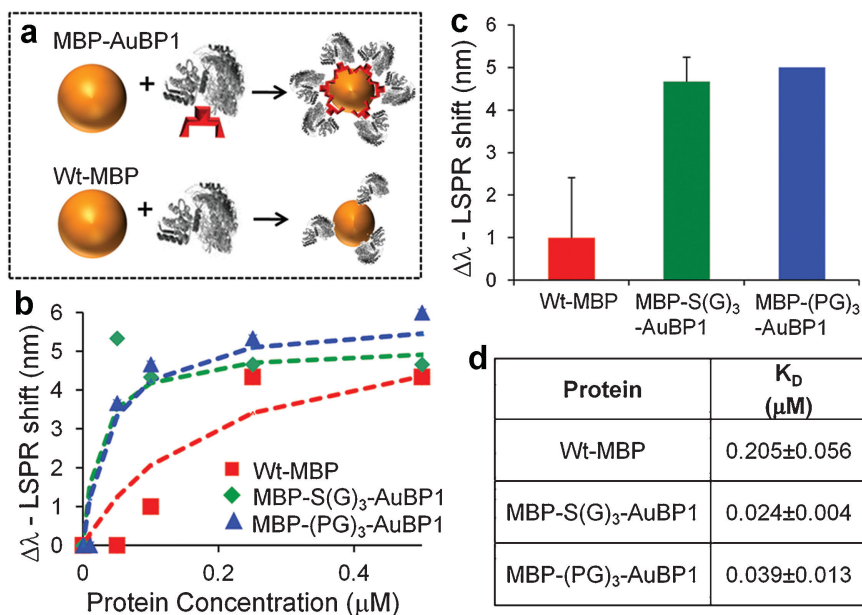


Figure 3. LSPR binding analysis and protein-functionalization of gold nanoparticles (Au NP). Schematic for functionalization of Au NP (**panel a**), LSPR shifts for fusion and wild type proteins plotted at various concentrations fitted with Langmuir curve (**panel b**); LSPR shifts for fusion and wild type proteins at 0.1 μ M concentration (**panel c**) and respective observed dissociation constants (K_D) (mean \pm SE) (**panel d**). [Color figure can be seen in the online version of this article, available at <http://wileyonlinelibrary.com/bit>]

affinity than either wt-MBP or bovine serum albumin (BSA) serving as controls (data not shown). In fact, observed LSPR shifts recorded for up to 0.1 μ M MBP-AuBP1 proteins show \sim 5–4 nm greater shift compared to control wt-MBP (Fig. 3c). Dissociation constants (K_D) were directly calculated by fitting Langmuir binding isotherm to the observed LSPR shifts via nonlinear curve fitting (Fig. 3b). Corresponding K_D values (mean \pm SE) for MBP-AuBP1 fusion proteins ($0.024 \pm 0.004 \mu\text{M}$ for MBP-S(G)₃-AuBP1 and $0.039 \pm 0.013 \mu\text{M}$ for MBP-(PG)₃-AuBP1) were found to be significantly lower than for wt-MBP protein ($0.205 \pm 0.056 \mu\text{M}$) (Fig. 3d and Supporting Information). The four- to sixfold decrease of observed dissociation constant for hetero-functional fusion proteins compared to wt-MBP is statistically significant at $\alpha = 0.05$ confirmed by the *t*-test and show outstanding correlation with calculated affinity constants observed in SPR binding assays. On the other hand, as with SPR results, we observed no statistically significant difference in binding affinity between the tested fusion proteins at $\alpha = 0.05$ in the *t*-test suggesting that both fusion proteins are equally functional. The detected enhanced binding affinities of the engineered MBP-AuBP1 proteins to the gold surfaces can be attributed to the AuBP1 peptide tag. Moreover, these findings suggest that the fusion MBP-AuBP1 proteins exhibit similar binding affinity to both flat planar and NP gold surface and that protein binding and self-assembly processes exhibit no or only negligible steric hindrance effect.

Stability and Surface Modifications of Hybrid MBP-AuBP1 Gold Nanoparticles

Previously it has been reported that Au NPs stabilized with loosely bound surfactants such as citrate, aggregate upon salt addition, for example, NaCl, due to the screening of the electrostatic repulsion between them (Levy et al., 2004). In salt-induced agglomeration assays, Au NP agglomeration is evidenced by a significant change in LSPR spectrum, such as decreased intensity for the characteristic LSPR band at \sim 520 nm and an increased absorption at longer wavelengths (\sim 650–700 nm) conveyed with corresponding color change from pink to blue. Here, we observe that the Au NP modified with fusion MBP-AuBP1 proteins exhibit exceptional stability and can withstand up to 0.5 M NaCl solution. In contrast, Au NP modified with wt-MBP protein aggregated at lower salt concentrations, as evidenced by solution color transition to blue and an appearance of large red-shifted absorption peak (Fig. 4a and Supporting Information). This result suggests that the bound wt-MBP protein is probably adhered to the Au surface with low binding strength as well as more random orientation, thus resulting in exposed surface of Au NP for interaction with salt ions promoting agglomeration.

These conclusions were further supported by experiments assaying protein-induced Au NP stability in gel electrophoresis (40 V) using low percentage of agarose gel of 0.5% (Fig. 4b and Supporting Information). In the agarose gel experiment, we observed significantly enhanced stability of

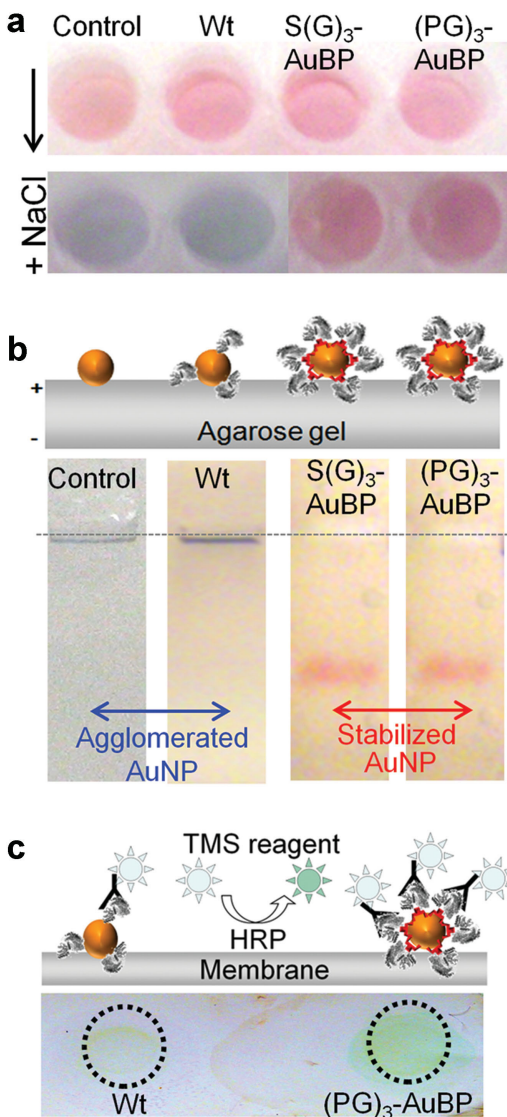


Figure 4. Stability of protein-functionalized gold nanoparticles. Images of functionalized Au NP with 1 μ M of either wt-MBP, MBP-AuBP1 derivatives and non-functionalized Au NP control before and after addition of 1 M NaCl (**panel a**); schematic cartoon for agarose gel electrophoresis of functionalized Au NP after functionalization reaction with 0.05 μ M proteins (**panel b**); immunoblotting onto nitrocellulose membrane using wt-MBP and MBP-(PG)₃-AuBP1 functionalized Au NP labeled with anti-MBP-HRP antibody and TMS substrate (**panel c**). [Color figure can be seen in the online version of this article, available at <http://wileyonlinelibrary.com/bit>]

Au NP functionalized with MBP-AuBP1 proteins which appeared as pink-colored bands, compared to agglomerated NP functionalized with wt-MBP and “bare” citrate-capped NP which appeared as blue-color bands in the agarose gel assay. We further demonstrated the enhanced surface modification induced by fusion MBP-AuBP1 proteins in simple blotting experiment on nitrocellulose membrane (Fig. 4c). The data shown in Figure 4c clearly demonstrate enhanced Au NP surface modification with fusion MBP-AuBP1 protein compared to wt-MBP control ([protein]

for both at 0.05 μ M). In summary, the observed NP characteristics, such as exceptional stability in the absence of excess capping ligand, as well as enhanced surface modifications induced by MBP-AuBP1, suggest that these functional Au NPs would be particularly suited for biological applications or for building nanostructures using biological interactions (Levy et al., 2004).

Fabrication of Protein Arrays Via Bio-Enabled Layer-by-Layer Self-Assembly

Recently protein arrays of controlled spatial distribution have been produced using various lithography techniques, including either soft-lithography (Qin et al., 2010; Xia and Whitesides, 1998), dip-pen lithography (Lee et al., 2002a; Piner et al., 1999), and photolithography (Blawas and Reichert, 1998) or by various immobilization chemistry (Nakanishi et al., 2008). By taking advantage of the high-affinity gold-binding capacity of AuBP1 peptide tag and high efficiency of conventional micro-contact printing technology (μ CP), we first demonstrate the fabrication of protein arrays on gold surfaces with enhanced molecular density in a single reaction step. As shown in Figure 5 (also see Supporting Information), fluorescence microscopy results of MBP-AuBP1 fusion protein arrays immunodetected by a specific anti-MBP-Alexa complex revealed enhanced binding of both MBP-AuBP1 fusion proteins compared to wt-MBP alone. It is apparent that MBP-AuBP1 protein assembles on gold surface with high molecular packing density and patterning efficiency evidenced by bright-, well-defined antibody-to-protein patterns (Fig. 5b–c). This result suggests that the specific AuBP1 epitope tags present in MBP-AuBP1 fusion proteins indeed control and direct the immobilization of fusion proteins onto the surface and represents an excellent interface for protein–surface interactions.

In our second approach, we fabricated a multilayered protein-Au NP arrays on a solid surface via a strategy using a combination of peptide-enabled layer-by-layer self-assembly and μ CP technique. Firstly, we produced novel hetero-functional peptide (QBP1-AuBP1) that includes both gold- and silica-binding motifs previously selected from combinatorial peptide libraries (Hnilova et al., 2008; Oren et al., 2007). By taking advantage of the multi-functional modality inherent to the designed QBP1-AuBP1 peptide, we fabricated Au NP arrays on top of the silica surface using a soft-lithography patterning technique as described in the “Materials and Methods” section of this manuscript and in Figure 6a. The detailed scans from atomic force microscopy, as well as images from dark field microscopy of Au NP patterns fabricated via hetero-functional QBP1-AuBP1 peptide linkage are given in Figure 6b–c. Collectively, AFM and DF data demonstrate that designed and engineered multi-functional QBP1-AuBP1 peptide can control the assembly of gold nanostructures on silica surfaces and, thus, can be used successfully to fabricate gold

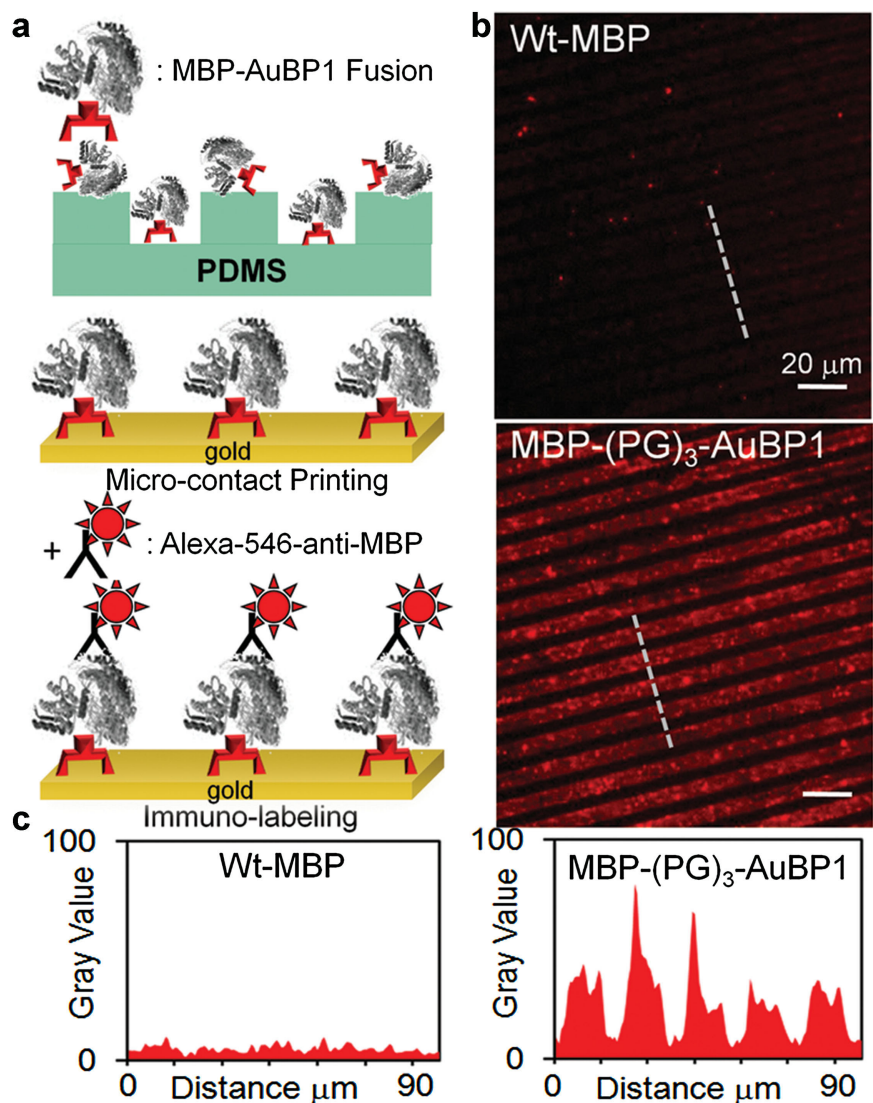


Figure 5. Controlled protein patterning on flat gold surface via micro-contact printing technique. Schematics of micro-contact printing and protein labeling (**panel a**); representative fluorescent images of 20 μM wt-MBP and MBP-(PG)₃-AuBP1 proteins labeled with anti-MBP-Alexa-546 antibody immobilized on planar gold surface using micro-contact printing (**panel b**); respective line scan plots of fluorescence images generated using ImageJ (NIH, Bethesda, MD) software (**panel c**). The protein-arrayed gold surfaces were imaged using a fluorescence microscope with corresponding fluorescent filter. The respective positions on fluorescence images used in ImageJ line scan analysis are indicated by dashed lines. [Color figure can be seen in the online version of this article, available at <http://wileyonlinelibrary.com/bit>]

nano particle arrays via a simple and robust protocol in aqueous solutions. In the next step the hetero-functional MBP-AuBP1 protein selectively immobilized onto Au NP arrays via of AuBP1 peptide tag through its high-affinity and specific interactions with Au surface. The immobilized MBP-AuBP1 fusion proteins were immuno-detected by a specific anti-MBP-Alexa complex. The fluorescence microscopy images shown in Figure 6c–d (see Supporting Information) confirm the high-affinity and material-selective self-assembly of MBP-AuBP1 fusion proteins onto Au NP, in a process resulting in the fabrication of spatially controllable multilayered protein arrays. In

contrast, wt-MBP protein did not reveal production of protein arrays and rather resulted in random non-specific immobilization of MBP onto both solid surfaces (Fig. 6c–d).

Conclusions

We describe herein a successful engineering and production of a hetero-functional protein unit containing two structural and functional domains; a MBP protein and a highly specific AuBP1 peptide-tag, originally selected from FliTrx peptide

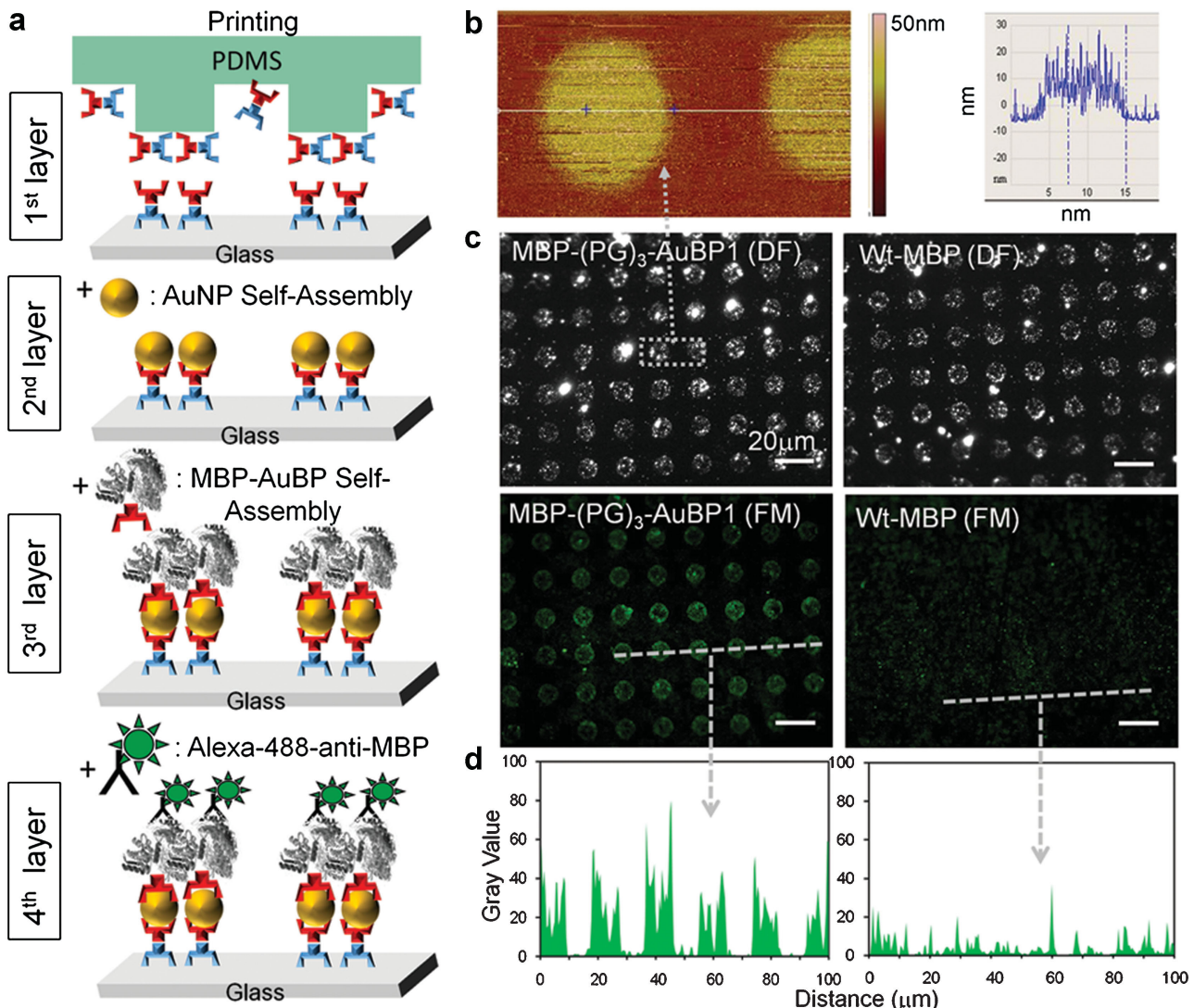


Figure 6. Layer-by-layer protein immobilization on Au NP-arrayed surface. Schematics of preparation of Au NP patterned surface by micro-contact printing and targeted protein immobilization on Au NP patterned surface by specific self-assembly (**panel a**); detail of atomic force microscopy scan of representative Au NP patterns immobilized on glass surface through QBP-PPP-AuBP bi-functional peptide (**panel b**); representative fluorescence and dark field images of 20 μM wt-MBP and MBP-(PG)₃-AuBP1 proteins immobilized on Au NP arrays labeled with anti-MBP-Alexa-488 antibody (**panel c**); corresponding line scan plots of fluorescence images generated using ImageJ software (NIH) (**panel d**). The protein molecules immobilized on Au NP arrayed surfaces were imaged using a fluorescence microscope with corresponding fluorescent filter. The respective positions on fluorescence images used in ImageJ line scan analysis are indicated by dashed lines. [Color figure can be seen in the online version of this article, available at <http://wileyonlinelibrary.com/bit>]

combinatorial library. In our design, the C'-terminally fused AuBP1 tag was separated from the MBP protein by two structurally different spacers, either a rigid (PGPGPG) or a flexible (SGGG) linker that provided further insights into the potential effect of spacers on the functionality of the fusion protein. Quantitative binding assays consisting of SPR and LSPR reveal that both engineered MBP-AuBP1 derivatives containing either proline-rich or glycine-rich linker preserved their gold-binding affinities as documented by their similar binding parameters and characteristics. This is probably related to the fusion construction parameters, C'-terminal genetic fusion as well as to the considerably

smaller size of AuBP1 tag peptide compared to MBP fusion partner.

Furthermore, the results demonstrate the utility of selective AuBP1 peptide tag that enables enhanced immobilization affinity and orientation of MBP-AuBP1 constructs on various gold surfaces using its exceptional molecular recognition and binding characteristics. Specifically, both of the engineered MBP-AuBP1 proteins demonstrated considerably higher binding affinities to various gold surfaces compared to wt-MBP as evidenced by nearly an order of magnitude enhanced binding parameters for MBP-AuBP1 fusions. Moreover we demonstrate that the novel peptide tag technology is highly

modular and versatile by designing a multi-functional QBP1-AuBP1 peptide for an addressed linkage of two different inorganic surfaces and effective bottom-up array fabrication. Collectively, we demonstrate that the effective short AuBP1 peptide tag can be successfully used in various arrangements, such as in hetero-functional peptides and proteins to facilitate effective bottom-up assembly of spatially distributed multilayer protein microarrays on metallic nanostructures on various solid supports.

This efficient and controlled layer-by-layer strategy for protein immobilization on micro- and nano-patterned surfaces may also be used for preparation of high-throughput LSPR or SERS biosensors with improved outcomes. As shown here, these peptide tags can concurrently direct, control and enhance the protein immobilization onto defined and specific solid surfaces. In contrast to conventional chemical and physical methods for protein adsorption, the robust peptide based approach described here is highly intriguing due to being relatively simple, biologically and environmentally friendly without the requirements of extreme chemical or physical conditions. Overall the results demonstrate that engineered peptides provide a viable alternative to the conventional chemical coupling to produce various protein and hybrid nanostructure assemblies with highly controllable organization and architecture. These layered architectures can be used in a wide range of practical applications, such as controlled bottom-up assembly of hybrid nanostructures, nanobio-photonics platforms and biosensing.

This work was supported by grants from NSF through the NSF-MRSEC Program through GEMSEC at UW (DMR#0520567) and Turkish State Planning Organization and TUBITAK/NSF-IRES joint project at ITU (BT; MH). The project was also partially supported by NSF-BioMat Program (DMR#0706655). The authors would like to thank Dr. T. Kacar for technical help and Prof. M. L. Snead for useful feedback on the manuscript. The research was carried out using facilities of GEMSEC (a part of MRFN) and CNT (a member of NNIN) at the UW.

References

- Anker JN, Hall WP, Lyandres O, Shah NC, Zhao J, Van Duyne RP. 2008. Biosensing with plasmonic nanosensors. *Nat Mater* 7(6):442–453.
- Blawas AS, Reichert WM. 1998. Protein patterning. *Biomaterials* 19(7-9):595–609.
- Boder ET, Wittrup KD. 1997. Yeast surface display for screening combinatorial polypeptide libraries. *Nat Biotechnol* 15(6):553–557.
- Boudou T, Crouzier T, Ren KF, Blin G, Picart C. 2010. Multiple functionalities of polyelectrolyte multilayer films: New biomedical applications. *Adv Mater* 22(4):441–467.
- Brown S, Sarikaya M, Johnson E. 2000. A genetic analysis of crystal growth. *J Mol Biol* 299(3):725–735.
- Brzoska JB, Benazouz I, Rondelez F. 1994. Silanization of solid substrates—A step towards reproducibility. *Langmuir* 10(11):4367–4373.
- Dai HX, Choe WS, Thai CK, Sarikaya M, Traxler BA, Baneyx F, Schwartz DT. 2005. Nonequilibrium synthesis and assembly of hybrid inorganic-protein nanostructures using an engineered DNA binding protein. *J Am Chem Soc* 127(44):15637–15643.
- Fairman R, Akerfeldt KS. 2005. Peptides as novel smart materials. *Curr Opin Struct Biol* 15(4):453–463.
- George RA, Heringa J. 2002. An analysis of protein domain linkers: Their classification and role in protein folding. *Protein Eng* 15(11):871–879.
- Hammond PT. 2004. Form and function in multilayer assembly: New applications at the nanoscale. *Adv Mater* 16(15):1271–1293.
- Hnilova M, Oren EE, Seker UOS, Wilson BR, Collino S, Evans JS, Tamerler C, Sarikaya M. 2008. Effect of molecular conformations on the adsorption behavior of gold-binding peptides. *Langmuir* 24(21):12440–12445.
- Iosin M, Toderas F, Baldeck PL, Astilean S. 2009. Study of protein-gold nanoparticle conjugates by fluorescence and surface-enhanced Raman scattering. *J Mol Struct* 924–926:196–200.
- Kacar T, Zin MT, So C, Wilson B, Ma H, Gul-Karaguler N, Jen AKY, Sarikaya M, Tamerler C. 2009. Directed self-immobilization of alkaline phosphatase on micro-patterned substrates via genetically fused metal-binding peptide. *Biotechnol Bioeng* 103(4):696–705.
- Khatayevich D, Gungormus M, Yazici H, So C, Cetinel S, Ma H, Jen A, Tamerler C, Sarikaya M. 2010. Biofunctionalization of materials for implants using engineered peptides. *Acta Biomater* 6(12):4634–4641.
- Krauland EM, Peelle BR, Wittrup KD, Belcher AM. 2007. Peptide tags for enhanced cellular and protein adhesion to single-crystal line sapphire. *Biotechnol Bioeng* 97(5):1009–1020.
- Kumara MT, Tripp BC, Muralidharan S. 2007. Self-assembly of metal nanoparticles and nanotubes on bioengineered flagella scaffolds. *Chem Mater* 19(8):2056–2064.
- Lee KB, Park SJ, Mirkin CA, Smith JC, Mrksich M. 2002a. Protein nanoarrays generated by dip-pen nanolithography. *Science* 295(5560):1702–1705.
- Lee SW, Mao CB, Flynn CE, Belcher AM. 2002b. Ordering of quantum dots using genetically engineered viruses. *Science* 296(5569):892–895.
- Levy R, Thanh NTK, Doty RC, Hussain I, Nichols RJ, Schiffrian DJ, Brust M, Fernig DG. 2004. Rational and combinatorial design of peptide capping ligands for gold nanoparticles. *J Am Chem Soc* 126(32):10076–10084.
- Mrksich M, Whitesides GM. 1996. Using self-assembled monolayers to understand the interactions of man-made surfaces with proteins and cells. *Annu Rev Biophys Biomol Struct* 25:55–78.
- Naik RR, Stringer SJ, Agarwal G, Jones SE, Stone MO. 2002. Biomimetic synthesis and patterning of silver nanoparticles. *Nat Mater* 1(3):169–172.
- Nakanishi K, Sakiyama T, Kumada Y, Imamura K, Imanaka H. 2008. Recent advances in controlled immobilization of proteins onto the surface of the solid substrate and its possible application to proteomics. *Current Proteomics* 5(3):161–175.
- Nath N, Chilkoti A. 2004. Label-free biosensing by surface plasmon resonance of nanoparticles on glass: Optimization of nanoparticle size. *Anal Chem* 76(18):5370–5378.
- Oren EE, Tamerler C, Sahin D, Hnilova M, Seker UOS, Sarikaya M, Samudrala R. 2007. A novel knowledge-based approach to design inorganic-binding peptides. *Bioinformatics* 23(21):2816–2822.
- Pacardo DB, Sethi M, Jones SE, Naik RR, Knecht MR. 2009. Biomimetic synthesis of Pd nanocatalysts for the Stille coupling reaction. *ACS Nano* 3(5):1288–1296.
- Park TJ, Zheng S, Kang YJ, Lee SY. 2009. Development of a whole-cell biosensor by cell surface display of a gold-binding polypeptide on the gold surface. *FEMS Microbiol Lett* 293(1):141–147.
- Piner RD, Zhu J, Xu F, Hong SH, Mirkin CA. 1999. “Dip-pen” nanolithography. *Science* 283(5402):661–663.
- Puurunen RL. 2005. Surface chemistry of atomic layer deposition: A case study for the trimethylaluminum/water process. *J Appl Phys* 97(12):52.
- Qin D, Xia YN, Whitesides GM. 2010. Soft lithography for micro- and nanoscale patterning. *Nat Protocols* 5(3):491–502.
- Rusmini F, Zhong ZY, Feijen J. 2007. Protein immobilization strategies for protein biochips. *Biomacromolecules* 8(6):1775–1789.
- Sano KI, Shiba K. 2003. A hexapeptide motif that electrostatically binds to the surface of titanium. *J Am Chem Soc* 125(47):14234–14235.
- Sarikaya M, Tamerler C, Jen AKY, Schulten K, Baneyx F. 2003. Molecular biomimetics: Nanotechnology through biology. *Nat Mater* 2(9):577–585.

- Schwartz DK, Garnaes J, Viswanathan R, Zasadzinski JAN. 1992. Surface order and stability of Langmuir–Blodgett films. *Science* 257(5069):508–511.
- Sedlak RH, Hnilova M, Gachelet E, Przybyla L, Dranow D, Gonon T, Sarikaya M, Tamerler C, Traxler B. 2010. An engineered DNA-binding protein self-assembles metallic nanostructures. *Chembiochem* 11(15):2108–2112.
- Sengupta A, Thai CK, Sastry MSR, Matthaei JF, Schwartz DT, Davis EJ, Baneyx F. 2008. A genetic approach for controlling the binding and orientation of proteins on nanoparticles. *Langmuir* 24(5):2000–2008.
- Seo HS, Kim SE, Park JS, Lee JH, Yang KY, Lee H, Lee KE, Han SS, Lee J. 2010. Three-dimensional nanostructured array of protein nanoparticles. *Adv Funct Mater* 20(23):4055–4061.
- Slocik JM, Naik RR, Stone MO, Wright DW. 2005. Viral templates for gold nanoparticle synthesis. *J Mater Chem* 15(7):749–753.
- Smith GP. 1985. Filamentous fusion phage—Novel expression vectors that display cloned antigens on the virion surface. *Science* 228(4705):1315–1317.
- Tamerler C, Oren EE, Duman M, Venkatasubramanian E, Sarikaya M. 2006. Adsorption kinetics of an engineered gold-binding peptide by surface plasmon resonance spectroscopy and a quartz crystal microbalance. *Langmuir* 22(18):7712–7718.
- Tamerler C, Khatayevich D, Gungormus M, Kacar T, Oren EE, Hnilova M, Sarikaya M. 2010. Molecular biomimetics: GEPI-based biological routes to technology. *Biopolymers* 94(1):78–94.
- Tang ZY, Wang Y, Podsiadlo P, Kotov NA. 2006. Biomedical applications of layer-by-layer assembly: From biomimetics to tissue engineering. *Adv Mater* 18(24):3203–3224.
- Tullman JA, Finney WF, Lin YJ, Bishnoi SW. 2007. Tunable assembly of peptide-coated gold nanoparticles. *Plasmonics* 2(3):119–127.
- Whaley SR, English DS, Hu EL, Barbara PF, Belcher AM. 2000. Selection of peptides with semiconductor binding specificity for directed nanocrystal assembly. *Nature* 405(6787):665–668.
- Wriggers W, Chakravarty S, Jennings PA. 2005. Control of protein functional dynamics by peptide linkers. *Biopolymers* 80(6):736–746.
- Xia YN, Whitesides GM. 1998. Soft lithography. *Annu Rev Mater Sci* 28:153–184.
- Yuca E, Karatas AY, Seker UOS, Gungormus M, Dinler-Doganay G, Sarikaya M, Tamerler C. 2011. In vitro labeling of hydroxyapatite minerals by an engineered protein. *Biotechnol Bioeng* 108(5):1021–1030.
- Zhen GL, Falconnet D, Kuennemann E, Voros J, Spencer ND, Textor M, Zurcher S. 2006. Nitrilotriacetic acid functionalized graft copolymers: A polymeric interface for selective and reversible binding of histidine-tagged proteins. *Adv Funct Mater* 16(2):243–251.
- Zheng S, Kim DK, Park TJ, Lee SJ, Lee SY. 2010. Label-free optical diagnosis of hepatitis B virus with genetically engineered fusion proteins. *Talanta* 82(2):803–809.